UDC 517.9

NONLINEAR VIBRATION SOLUTION OF AN INCLINED TIMOSHENKO BEAM UNDER THE ACTION OF A MOVING FORCE WITH CONSTANT/NON-CONSTANT VELOCITY

НЕЛІНІЙНІ ВІБРАЦІЙНІ РОЗВ'ЯЗКИ НАХИЛЕНОЇ БАЛКИ ТИМОШЕНКА ПІД ДІЄЮ РУХОМОЇ СИЛИ ЗІ СТАЛОЮ АБО ЗМІННОЮ ШВИДКІСТЮ

A. Mamandi

Parand Branch, Islamic Azad Univ., Tehran, Iran
e-mail: am_2001h@yahoo.com

M. H. Kargarnovin

Sharif Univ. Technology, Tehran, Iran

S. Farsi

Tarbiat Modares Univ., Tehran, Iran

This study focuses on the nonlinear dynamic response of an inclined Timoshenko beam with different boundary conditions subjected to a moving force under the influence of three types of motions, including accelerating, decelerating and constant velocity types of motion, respectively. The beam's nonlinear governing coupled partial differential equations (PDEs) of motion for the bending rotation of warped cross-section, longitudinal and transverse displacements are derived using Hamilton's principle. To obtain the dynamic response of the beam under the action of a moving force, the derived nonlinear coupled PDEs of motion are solved by applying Galerkin's method. Then the beam's dynamic response is obtained using mode summation technique. Furthermore, the calculated results are verified with those obtained by finite element method (F.E.M.) analysis. In the next step a parametric study on the response of the beam is conducted by changing the magnitude of the traveling concentrated force, its velocity and beam's boundary conditions and likewise their sensitivity on the beam's dynamic response are studied, respectively. It is observed that the existence of quadratic-cubic nonlinearity in the governing coupled PDEs of motion renders hardening/softening behavior on the dynamic response of the beam. Moreover, it is noticed that any restriction on the beam mid-plane stretching will introduce nonlinear behavior in the beam's PDEs of motion.

Вивчено нелінійну динамічну реакцію нахиленої балки Тимошенка з різними граничними умовами під дією рухомої сили, включаючи вплив рухів трьох типів, зокрема руху з прискоренням, уповільненням та сталою швидкістю. З допомогою принципу Гамільтона отримано нелінійні зв'язані рівняння з частинними похідними для вигину обертання деформованого перетину, поздовжнього та поперечного зсувів. Для встановлення динамічної реакції балки під дією рухомої сили було розв'язано отримані нелінійні зв'язані рівняння з використанням методу Гальоркіна. Далі динамічну реакцію балки було одержано з використанням техніки модального підсумовування. Встановлені результати було перевірено за допомогою методу скінченних елементів. На наступному кроці було проведено параметричний аналіз реакції балки при зміні величини рухомої концентрованої сили, її швидкості та граничних умов, а також чутливості реакції балки на ці параметри. Було помічено, що наявність квадратичної або кубічної нелінійності у зв'язаних рівняннях з частинними похідними робить динамічну реакцію балки більш твердою

або м'якою, а будь-які обмеження на розтягування середньої площини вводять нелінійність у рівняння руху балки.

1. Introduction. Under actual operating conditions, the linear and nonlinear vibration analysis of structural elements, such as strings, rods, beams, plates and shells traveling by a moving mass/force is of considerable practical importance to the structural and railway engineers. For over a century many analytical and numerical methods have been proposed to investigate the dynamic behavior of different engineering structures. However, until now almost no attention has been paid to the study of nonlinear dynamic analysis for the coupled bending rotation of the warped cross-section, longitudinal and transverse deflections of an inclined Timoshenko beam subjected to a moving force. Some practical examples for such behavior are a bridge when traveled by moving vehicles or trains, an overhead traveling crane moving on its girder, a beam subjected to pressure waves, simulation of high axial speed machining operations and internal two-phase flow in piping systems. Further application on the subject of vibrations of the inclined beams can be addressed in the aerospace and armed force industries such as rocket launcher systems and cannon tubes.

It should be emphasized that from a mechanical component design point of view, inclusion of acceleration/deceleration character of moving mass/force certainly plays a significant role in the final results. This becomes more critical when one deals, for example, with take-off and landing phase of aircrafts on runways/angle decks (flight decks) of warship aircraft carriers, automobiles and locomotives at take off or sudden brake on roadways/highway bridges and on rails/railway bridges, respectively. Furthermore, frequent braking and accelerating of rail-guided cranes play important role in design steps of these types of structures.

Related to the vibration analysis of Euler – Bernoulli beam either under motion of traveling force or traveling mass numerous works are reported [1 – 12]. Similarly, one can find number of different studies on the dynamical behavior of Timoshenko beams subjected to motion of moving load and mass [7, 10, 11, 13 – 18]. Nonlinear dynamic analysis of Euler – Bernoulli and Timoshenko beams under the action of either moving force or mass are specifically investigated in [4, 8, 9, 12, 14, 16 – 18].

From the experimental point of view, it appears that as the amplitude of vibration increases, nonlinear effects come into play; therefore by considering that the source of nonlinearity may be either inertial, geometric or material in nature, the influence of such terms on the beam dynamic behavior should also be included (see Refs. [8, 14, 19]). In this paper, attention is paid to geometric nonlinearity which may be caused by large curvatures and nonlinear stretching of the mid-plane of an inclined Timoshenko beam. In general, due to existence of nonlinear terms, the exact analytical (closed form) solutions for governing equations of motion are not available.

In this study three nonlinear governing coupled PDEs of motion for the bending rotation of warped cross-section, transverse and longitudinal vibrations of an inclined Timoshenko beam under the action of a moving force are derived using Hamilton's principle. Then by applying Galerkin's method three obtained nonlinear second order ordinary differential equations (ODEs) governing modal equations can be solved numerically using the *Adams – Bashforth – Moulton* integration method via MATLAB solver package. It should be noted that in the present study the nonlinear effects of axial strain, bending curvature and shear strain on the dynamic responses of the inclined Timoshenko beam are all considered using the von-Karman strain-displacement relation in conjunction with the moderately large deflection theory.

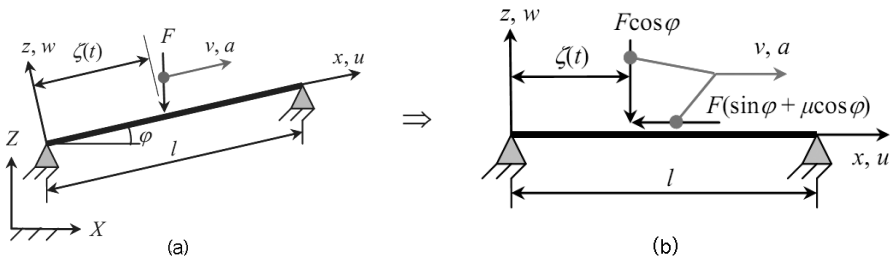

Fig. 1. (a) A lateral force traveling on an inclined pinned-pinned beam. (b) Acting forces on the elastic beam at the contact point in the equivalent moving force model.

In extending the issue of moving mass further to a more applicable study we believe that the same problem but under motion of the moving force has its own importance in this filed. Based on this postulate and on the same line to the other studies by the same authors [18] this study is initiated. It should be mentioned that there is not going to be any novelty on the solution technique in this paper with respect to the some previous works but what makes this work new is related to the very important outcome results from the application point of view. Briefly, it should be pointed out that the main contribution and significant technical advantages of this paper is to present some tangible results which have not been reported in the earlier published papers.

2. Mathematical modeling. An inclined Timoshenko beam with length l and inclination angle φ traveled by a concentrated force F with velocity v and constant acceleration/deceleration a is considered (see Fig. 1(a)). The longitudinal and lateral components of the force with which the traveling force acts on the beam are $F\cos\varphi$ and $F(\sin\varphi+\mu\cos\varphi)$, respectively, as shown in Fig. 1(b). In our upcoming analysis, when the load enters the left end of the beam, zero initial conditions for the beam are assumed, i.e., the beam is at rest at time $t = 0$. It is further assumed that the external damping is not negligible and the damping behavior follows the viscous nature [2, 8, 10, 11]. Moreover, the beam deforms within the linear elastic range and therefore Hooke's laws are prevailing. In this study the von-Karman's moderately large strain-displacement relations are used as [14, 18]:

$$\varepsilon_{xx} = u_{,x} + \frac{1}{2}w_{,x}^2, \quad w_{,x} = \psi + \gamma \quad \text{and} \quad \kappa = \psi_{,x} \tag{1}$$

in which $u = u(x,t)$ is the axial longitudinal time-dependent in-plane displacement, $w = w(x,t)$ is the time-dependent transverse deflection of the beam measured upward from its equilibrium position when unloaded and $\psi = \psi(x,t)$ is the time-dependent rotation of the warped cross-section of the beam due to the bending. The subscripts $(,t)$ and $(,x)$ stand for the derivative with respect to the time (t) and spatial coordinate (x) to the related order, respectively. In addition, ε, γ and κ are the longitudinal (or normal) strain, shear strain and curvature at the center line of the Timoshenko beam, respectively. To obtain the governing differential equations of motion by applying Hamilton's principle the kinetic energy, K, and the strain

energy, U, of the beam are:

$$K = \frac{1}{2}\left(\int_0^l \rho A w_{,t}^2\,dx + \int_0^l \rho A u_{,t}^2\,dx + \int_0^l \rho I_d {\psi_{,t}}^2\,dx\right), \tag{2a}$$

$$U = \frac{1}{2}\left(\int_0^l EA\varepsilon_{xx}^2\,dx + \int_0^l EI_d\kappa^2\,dx + \int_0^l kGA\gamma^2\,dx\right). \tag{2b}$$

The total external virtual work done by the traveling force with variable velocity, frictional force and external viscous damping forces acting on the beam is:

$$\delta W_e = -\int_0^l \left(F(\sin\varphi + \mu\cos\varphi)\delta u + F\cos\varphi\delta w + c_1\psi_{,t}\delta\psi + c_2 w_{,t}\delta w + c_3 u_{,t}\delta u\right)\big|_{x=\zeta(t)}\,dx \tag{3}$$

in which $c_1\psi_{,t}$, $c_2 w_{,t}$ and $c_3 u_{,t}$ are regarded as the external viscous damping forces applied on the beam [2, 8–11]. Now, we can establish the Lagrangian function of the system as: $L = K - (U - W_e)$. Applying Hamilton's principle on L as: $\delta\int_{t_1}^{t_2} L\,dt = 0$ or

$$\delta\int_{t_1}^{t_2}(U-K)\,dt = \int_{t_1}^{t_2}\delta W_e\,dt. \tag{4}$$

By doing some mathematics, one would get the nonlinear governing coupled PDEs of motion (EOMs) as well as the boundary conditions (BCs) for the problem at hand as follows:
the moment relation in ψ direction,

$$\rho I_d\psi_{,tt} - EI_d\psi_{,xx} - kGA(w_{,x} - \psi) + c_1\psi_{,t} = 0, \tag{5}$$

the force relation in z direction,

$$\rho A w_{,tt} + kGA\left(\psi_{,x} - w_{,xx}\right) - EA\left(u_{,xx}w_{,x} + u_{,x}w_{,xx} + \frac{3}{2}\,w_{,xx}w_{,x}^2\right) + \\ + c_2 w_{,t} = -F\cos\varphi\delta(x - \zeta(t))\chi(t), \tag{6}$$

the force relation in x direction:

$$\rho A u_{,tt} - EA(u_{,xx} + w_{,x}w_{,xx}) + c_3 u_{,t} = -F(\sin\varphi + \mu\cos\varphi)\delta\left(x - \zeta(t)\right)\chi(t), \tag{7}$$

and the boundary conditions at both ends for the Timoshenko beam are

i- either $M = EI_d\psi_{,x}$ or ψ prescribed; (8a)

ii- either $Q = kGA(w_{,x} - \psi) + EA\left(u_{,x}w_{,x} + \frac{1}{2}\,w_{,x}^3\right)$ or w prescribed; (8b)

iii- either $N = EA\left(u_{,x} + \frac{1}{2}\,w_{,x}^2\right)$ or u prescribed, (8c)

where ρ is the beam density, A is the cross-sectional area of the beam, I_d is the beam's cross-sectional second moment of inertia, E is Young's modulus of elasticity, G is the shear modulus, k is the shear correction factor, EI_d is the beam's flexural rigidity, ρA is the beam's mass per unit length, F is the magnitude of the traveling force, μ is the kinetic frictional coefficient, c_1, c_2 and c_3 are external damping constants related to viscous damping of the beam, namely η, also M, Q and N are the bending (flexural) moment, shear force and axial (longitudinal) tension/compression force of the beam, respectively. Furthermore, $\delta(x-\zeta(t))$ is Dirac's delta function in which $\zeta(t)$ is the instantaneous position of the moving force with the velocity v and constant acceleration/deceleration a on the beam such that $\zeta(t)=x_0+vt$ or $\zeta(t)=x_0+vt+$ $+1/2at^2$ for describing the constant velocity or accelerating/decelerating types of motion of the traveling force, respectively, where x_0 is the initial point of application of the force on the beam, v is the traveling force entrance/exit velocity and a is the constant acceleration/deceleration of traveling force on the beam, $\chi(t)$ is the pulse function which is equal to one while the force is traveling on the beam, and zero when the traveling force is outside the beam span; for example in the case of constant velocity type of motion that is described by $\chi(t)=u(t)-u(t-l/v)$, in which $u(t)$ represents the unit step function. The derivation of nonlinear governing coupled PDEs of motion is rather lengthy and for brevity its details will not be given here.

3. Solution method. In this study Galerkin's method is chosen as a powerful computational tool to analyze the vibrations of an inclined Timoshenko beam. Based on the separation of variables technique, the response of Timoshenko beam in terms of the linear free-oscillation modes can be assumed as follows [18, 21]:

$$w(x,t)=\sum_{j=1}^{n}\phi_j(x)p_j(t)=\mathbf{\Phi}^T(x)\mathbf{P}(t), \tag{9}$$

$$\psi(x,t)=\sum_{j=1}^{n}\tau_j(x)q_j(t)=\mathbf{\Gamma}^T(x)\mathbf{Q}(t), \tag{10}$$

$$u(x,t)=\sum_{j=1}^{n}\theta_j(x)r_j(t)=\mathbf{\Theta}^T(x)\mathbf{R}(t), \tag{11}$$

where $\mathbf{P}(t)$, $\mathbf{Q}(t)$ and $\mathbf{R}(t)$ are vectors of order n listing the generalized coordinate $p_j(t)$, $q_j(t)$ and $r_j(t)$, respectively, and $\mathbf{\Phi}(x)$, $\mathbf{\Gamma}(x)$ and $\mathbf{\Theta}(x)$ are some vector functions collecting the first n mode shapes (eigen-functions) of $\phi_j(x)$, $\tau_j(x)$ and $\theta_j(x)$, respectively.

By substituting Eqs. (9), (10) and (11) into Eqs. (5), (6) and (7), pre-multiplying both sides of Eqs. (5), (6) and (7) by $\mathbf{\Gamma}^T(x)$, $\mathbf{\Phi}^T(x)$ and $\mathbf{\Theta}^T(x)$, respectively, integrating over the interval $(0,l)$ and imposing the properties of the Dirac's delta function, the resulting nonlinear coupled modal equations of motion in matrix form are as follows:

$$\rho I_d\sum_{j=1}^{n}\mathbf{S}_{ij}\ddot{q}_j(t)+2\rho I_d\eta\omega_i\sum_{j=1}^{n}\mathbf{S}_{ij}\dot{q}_j(t)-\sum_{j=1}^{n}\left[EI_d\mathbf{K}_{ij}-kGA\mathbf{S}_{ij}\right]q_j(t)-$$

$$-kGA\sum_{j=1}^{n}\mathbf{E}_{ij}p_j(t)=0, \tag{12}$$

$$\rho A\sum_{j=1}^{n}\mathbf{M}_{ij}\ddot{p}_j(t)+2\rho A\eta\omega_i\sum_{j=1}^{n}\mathbf{M}_{ij}\dot{p}_j(t)-kGA\sum_{j=1}^{n}\mathbf{H}_{ij}p_j(t)+kGA\sum_{j=1}^{n}\mathbf{F}_{ij}q_j(t)-$$

$$-EA\sum_{j=1}^{n}\sum_{k=1}^{n}r_j(t)\mathbf{G}_{ijk}p_k(t)-EA\sum_{j=1}^{n}\sum_{k=1}^{n}p_j(t)\mathbf{T}_{ijk}r_k(t)-$$

$$-\frac{3}{2}EA\sum_{j=1}^{n}\sum_{k=1}^{n}p_j(t)\mathbf{I}_{ijk}p_k(t)^2=-F\cos\varphi\chi(t)\mathbf{b}_i(t), \tag{13}$$

and

$$\rho A\sum_{j=1}^{n}\mathbf{J}_{ij}\ddot{r}_j(t)+2\rho A\eta\lambda_{li}\sum_{j=1}^{n}\mathbf{J}_{ij}\dot{r}_j(t)-EA\sum_{j=1}^{n}\mathbf{N}_{ij}r_j(t)-$$

$$-EA\sum_{j=1}^{n}\sum_{k=1}^{n}p_j(t)\mathbf{L}_{ijk}p_k(t)=-F\left[\sin\varphi+\mu\cos\varphi\right]\chi(t)\mathbf{d}_i(t) \tag{14}$$

for $i=1,2,\ldots,n$, in which the matrices $\mathbf{S}$, $\mathbf{K}$, $\mathbf{L}$, $\mathbf{M}$, $\mathbf{N}$, $\mathbf{I}$, $\mathbf{J}$, $\mathbf{T}$, $\mathbf{E}$, $\mathbf{F}$, $\mathbf{G}$ and $\mathbf{H}$ are defined as:

$$(\mathbf{M})_{ij}=\int_0^l\phi_i(x)\phi_j(x)\,dx,\quad(\mathbf{H})_{ij}=\int_0^l\phi_i(x)\phi_j''(x)\,dx,$$

$$(\mathbf{F})_{ij}=\int_0^l\phi_i(x)\tau_j'(x)\,dx,\quad(\mathbf{S})_{ij}=\int_0^l\tau_i(x)\tau_j(x)\,dx,$$

$$(\mathbf{K})_{ij}=\int_0^l\tau_i(x)\tau_j''(x)\,dx,\quad(\mathbf{E})_{ij}=\int_0^l\tau_i(x)\phi_j'(x)\,dx,$$

$$(\mathbf{J})_{ij}=\int_0^l\theta_i(x)\theta_j(x)\,dx,\quad(\mathbf{N})_{ij}=\int_0^l\theta_i(x)\theta_j''(x)\,dx,$$

$$(\mathbf{G})_{ijk}=\int_0^l\phi_i(x)\theta_j''(x)\phi_k'(x)\,dx,\quad(\mathbf{I})_{ijk}=\int_0^l\phi_i(x)\phi_j''(x)\phi_k'^{\,2}(x)\,dx,$$

$$(\mathbf{L})_{ijk}=\int_0^l\theta_i(x)\phi_j''(x)\phi_k'(x)\,dx,\quad(\mathbf{T})_{ijk}=\int_0^l\phi_i(x)\phi_j''(x)\theta_k'(x)\,dx, \tag{15}$$

where $i,j,k=1,2,3,\ldots,n$.

Prime and dot marks over any parameter indicate the derivative with respect to the position (x) and time (t), respectively. Furthermore, the $n \times 1$ column vectors of $\mathbf{b}$ and $\mathbf{d}$ are defined as

$$(\mathbf{b})_i = \phi_i\left(x = \zeta(t)\right) \quad \text{and} \quad (\mathbf{d})_i = \theta_i\left(x = \zeta(t)\right). \tag{16}$$

It is clear that Eqs. (12), (13) and (14) are three nonlinear coupled second-order ordinary differential equations (ODEs). The boundary conditions for a pinned-pinned Timoshenko beam with fixed end supports are [18, 20, 21]:

$$\begin{gathered}\text{essential BCs}: \begin{cases} u(0,t) = u(l,t) = 0 \Rightarrow \theta_j(x) = 0 & \text{at} \quad x = 0 \quad \text{and} \quad l, \\ w(0,t) = w(l,t) = 0 \Rightarrow \phi_j(x) = 0 & \text{at} \quad x = 0 \quad \text{and} \quad l; \end{cases} \\ \text{natural BCs}: M(0,t) = M(l,t) = 0 \Rightarrow \tau_{j,x}(x) = 0 \quad \text{at} \quad x = 0 \quad \text{and} \quad l. \end{gathered} \tag{17}$$

The boundary conditions for a clamped-pinned Timoshenko beam with immovable end supports are [18, 20, 21]:

$$\begin{gathered}\text{essential BCs}: \begin{cases} u(0,t) = u(l,t) = 0 \Rightarrow \theta_j(x) = 0 & \text{at} \quad x = 0 \quad \text{and} \quad l, \\ w(0,t) = w(l,t) = 0 \Rightarrow \phi_j(x) = 0 & \text{at} \quad x = 0 \quad \text{and} \quad l, \\ \psi(0,t) = 0 \Rightarrow \tau_j(x) = 0 & \text{at} \quad x = 0; \end{cases} \\ \text{natural BCs}: M(l,t) = 0 \Rightarrow \tau_{j,x}(x) = 0 \quad \text{at} \quad x = l. \end{gathered} \tag{18}$$

And the boundary conditions for a clamped-free Timoshenko beam are as follows [18, 20, 21]:

$$\begin{gathered}\text{essential BCs}: \begin{cases} u(0,t) = 0 \Rightarrow \theta_j(x) = 0 & \text{at} \quad x = 0, \\ w(0,t) = 0 \Rightarrow \phi_j(x) = 0 & \text{at} \quad x = 0, \\ \psi(0,t) = 0 \Rightarrow \tau_j(x) = 0 & \text{at} \quad x = 0; \end{cases} \\ \text{natural BCs}: \begin{cases} M(l,t) = 0 \Rightarrow \tau_{j,x}(x) = 0 & \text{at} \quad x = l, \\ Q(l,t) = 0 \Rightarrow kGA(w_{,x} - \psi) = 0 & \text{at} \quad x = l, \\ N(l,t) = 0 \Rightarrow EA(u_{,x}) = 0 & \text{at} \quad x = l. \end{cases} \end{gathered} \tag{19}$$

Moreover, Initial Conditions (ICs) for the Timoshenko beam are

$$\text{ICs}: u(x,0) = u_{,t}(x,0) = w(x,0) = w_{,t}(x,0) = \psi(x,0) = \psi_{,t}(x,0) = 0. \tag{20}$$

In Eq. (14), λ_{li} denotes the natural angular frequency (rad/s) of longitudinal vibration of the beam related to its type of boundary condition. For the either pinned-pinned or clamped-pinned beam it is in the form of $\dfrac{i\pi}{l}\sqrt{E/\rho}$ [18, 20, 21], and for a cantilever beam is given by $\dfrac{(2i-1)\pi}{2l}\sqrt{E/\rho}$ [18, 20, 21], where $i = 1, 2, 3, \ldots, n$.

To solve Eqs. (12), (13) and (14), all entries in the matrices in Eqs. (15) and (16) should be calculated. Herein, by inspection it can be seen that the following functions (mode shapes) for $\phi_j(x)$, $\tau_j(x)$ and $\theta_j(x)$ will satisfy both the linearized equations of motion of the beam and different types of boundary conditions as the following [13, 18, 20, 21]:

(i) For a pinned-pinned Timoshenko beam, the normal modes are expressed as follows:

$$\begin{aligned} \phi_j(x) &= D\sin(bB\xi), \\ \tau_j(x) &= H\cos(bB\xi), \\ \text{and} \quad \theta_j(x) &= \sin(j\pi\xi), \quad \xi = \frac{x}{l}, \quad \text{with} \quad j = 1, 2, 3, \ldots, n, \end{aligned} \tag{21a}$$

in which the frequency equation is

$$\sin bB = 0, \tag{21b}$$

where, in this case, $\sin bB = n\pi$, with $n = 1, 2, 3, \ldots$.

(ii) For a clamped-pinned Timoshenko beam, the normal modes are

$$\begin{aligned} \phi_j(x) &= D[\cosh bA\xi - \coth bA \sinh bA\xi - \cos bB\xi + \cot bB \sin bB\xi], \\ \tau_j(x) &= H\left[\cosh bA\xi + \frac{\sigma}{\lambda Z}\sinh bA\xi - \cos bB\xi + \sigma \sin bB\xi\right], \\ \text{and} \quad \theta_j(x) &= \sin(j\pi\xi), \quad \xi = \frac{x}{l}, \quad \text{with} \quad j = 1, 2, 3, \ldots, n, \end{aligned} \tag{22}$$

in which the frequency equation is

$$\lambda Z \tanh bA - \tan bB = 0. \tag{23}$$

(iii) For a clamped-free Timoshenko beam, the normal modes are

$$\begin{aligned} \phi_j(x) &= D[\cos bA\xi - \lambda Z\Delta \sinh bA\xi - \cos bB\xi + \Delta \sin bB\xi], \\ \tau_j(x) &= H\left[\cosh bA\xi + \frac{\sigma}{\lambda Z}\sinh bA\xi - \cos bB\xi + \sigma \sin bB\xi\right], \\ \text{and} \quad \theta_j(x) &= \sin[(j-1/2)\pi\xi], \quad \xi = \frac{x}{l}, \quad \text{with} \quad j = 1, 2, 3, \ldots, n, \end{aligned} \tag{24}$$

in which the frequency equation is given by

$$2 + [b^2(r^2 - s^2)^2 + 2]\cosh bA \cos bB - \frac{b(r^2 + s^2)}{(1 - b^2r^2s^2)^{1/2}}\sinh bA \sin bB = 0, \tag{25}$$

where, in Eqs. (21) – (25),

$$\begin{aligned} b^2 &= \frac{\rho A l^4}{EI_d}\omega^2, \quad r^2 = \frac{I_d}{Al^2}, \quad s^2 = \frac{EI_d}{kGAl^2}, \quad Z = \frac{B^2 - s^2}{A^2 + s^2}, \quad \lambda = \frac{A}{B}, \\ A, B &= \frac{1}{\sqrt{2}}\left\{\mp(r^2 + s^2) + [(r^2 - s^2)^2 + \frac{4}{b^2}]^{\frac{1}{2}}\right\}^{\frac{1}{2}}, \\ \sigma &= -\frac{\lambda \sinh bA + \sin bB}{\frac{1}{Z}\cosh bA + \cos bB}, \quad \Delta = \frac{\frac{1}{\lambda}\sinh bA - \sin bB}{Z\cosh bA + \cos bB}, \end{aligned} \tag{26}$$

in which D_i and H_i, $i = 1, 2, 3, \ldots, n$, are normal modal amplitudes which depend on natural frequencies of the Timoshenko beam related to the type of BCs. Moreover, it should be pointed out that ω_i is the natural angular frequency (rad/s) of transversal/bending slope warping vibration of the beam which depends on the type of boundary condition and can be obtained from Eq. (26) [18, 20].

By inserting the corresponding normal modes for any type of boundary condition of the beam into the Eqs. (15) and (16) all entries in all matrices can be calculated. In the next step these evaluated matrices will be inserted in the Eqs. (12), (13) and (14) and the later set of equations can be solved numerically using the *Adams–Bashforth–Moulton* integration method via MATLAB solver package out of which the values of $p_n(t)$, $q_n(t)$ and $r_n(t)$ can be obtained. By back substitution of $p_n(t)$, $q_n(t)$ and $r_n(t)$ in Eqs. (9), (10) and (11), $u(x,t)$, $w(x,t)$ and $\psi(x,t)$ are established, respectively [18, 21].

In the next step based on the obtained values for $u(x,t)$, $w(x,t)$ and $\psi(x,t)$, the dynamic response of an inclined Timoshenko beam having three different types of boundary conditions including pinned-pinned, clamped-pinned and clamped-free under influence of three types of force motions of a) accelerating, b) decelerating and c) uniform velocity motion are obtained. The obtained results for the beam response under each of those three types of force motions and boundary conditions are shown separately in the Figs. 4 to 14. The detailed kinematical discussions of the above different motions are described below [18].

a) In the case of constant accelerating type of motion ($\zeta(t) = x_0 + v_0 t + 1/2at^2$, $a = \mathrm{const} > 0$), it is assumed that the beam is at rest when the force F enters the beam at $x_0 = 0$ and $t_0 = 0$ with initial velocity $v_0 = 0$ and it arrives to the other end of the beam, i.e., $x = l$ with final velocity v. The total traveling time in the beam span, t_1, and force exit velocity v will be:

$$t_1 = \frac{2l}{v}, \tag{27a}$$

$$v = \sqrt{2al}. \tag{27b}$$

b) For constant decelerating type of motion ($\zeta(t) = x_0 + v_0 t + 1/2at^2$, $a = \mathrm{const} < 0$), it is also assumed that the beam is at rest when the force F enters the beam at $x_0 = 0$ and $t_0 = 0$ with entrance velocity v_0 (non-zero initial velocity) and it stops ($v = 0$) at the other end of the beam, i.e., $x = l$. The total traveling time in the beam span, t_2, and force entrance velocity v_0 will be:

$$t_2 = \frac{2l}{v_0}, \tag{28a}$$

$$v_0 = \sqrt{2l|a|}. \tag{28b}$$

c) For uniform velocity type of motion ($\zeta(t) = x_0 + v_0 t$, $v_0 = \mathrm{const} > 0$), it is also assumed that the beam is at rest when the force F enters the beam at $x_0 = 0$ and $t_0 = 0$ with force constant velocity v_0 and it reaches to the other end of the beam, i.e., $x = l$ at instant t_3. The total traveling time in the beam span, t_3 will be:

$$t_3 = \frac{l}{v_0}. \tag{29}$$

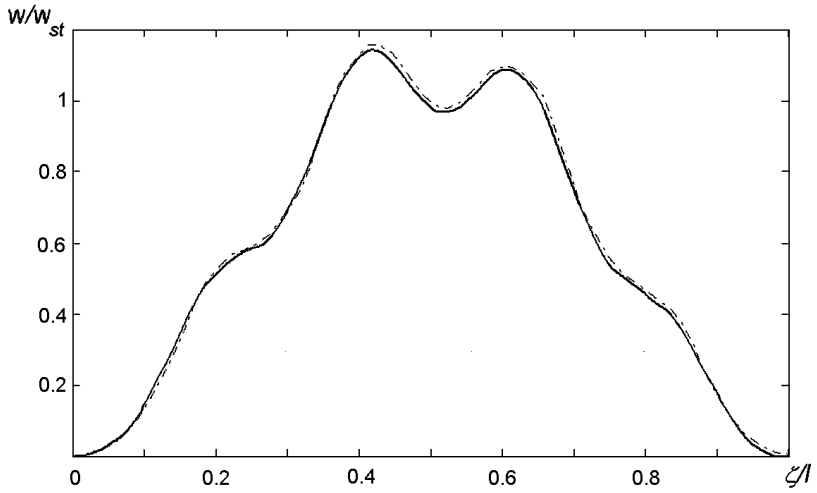

Fig. 2. Instantaneous normalized vertical displacement under a moving force of F, (—) linear analysis using present study, (– · –) linear analysis: Ref [13].

4. Verification of results and case studies. As mentioned in the introduction at the moment no specific results exist for the problem under consideration in the literature. Therefore, to verify the validity of the obtained results in this study we have to consider some special cases of our study to be compared with those existing in the literatures.

4.1. Verification of results in the linear case. In the first attempt we set the higher order terms, i.e., $\left(u_{,xx}w_{,x} + u_{,x}w_{,xx} + \frac{3}{2}w_{,xx}{w_{,x}}^2\right)$ and $(u_{,xx} + w_{,x}w_{,xx})$ of the left-hand sides of Eqs. (6) and (7), respectively, equal to zero for a constant velocity type of motion ($a = 0$). Furthermore, referring to Eqs. (12) to (14) we set: $c_1 = c_2 = c_3 = 0$, i.e., $\eta = 0$, $\mu = 0$ and $\varphi = 0$. This led us to a set of relations for $u(x,t)$, $w(x,t)$ and $\psi(x,t)$ referring to the case known for linear analysis for a horizontal undamped Timoshenko beam. To establish verifications of our analysis, we consider the data given in [13] as: $l = 1\,m$, $E = 207 \times 10^9\,N/m^2$, $G = 77.6 \times$ $\times 10^9\,N/m^2$, $k = 0.9$, $\rho = 7700\,kg/m^3$, $I_d = 6.236 \times 10^{-5}\,m^4$, $A = 0.02736\,m^2$, $F = 0.2\rho g \times$ $\times Al(N)$, $\alpha = 0.11$ and $\beta_0 = 0.15$, in which $\beta_0 = \pi r_0/l$ is Rayleigh's slenderness coefficient with r_0 taken as the radius of gyration of the beam. Based on the above data, the computer code was run for the linear case, and the vertical displacement (w) of the instantaneous positions of the moving force is calculated and the dimensionless outcome results are depicted and compared with other existing results in Fig. 2. The normalization factor for the vertical displacement is $w_{st} = Fl^3/48EI_d$, which is a mid point deflection of a simply supported beam under mid-span concentrated load of F. A close inspection of the curves in the Fig. 2 indicates good agreements between the two results.

4.2. Verification of results in the nonlinear case. As described earlier, in this study to extend the validity of our obtained results we prepared appropriate APDL (ANSYS Parametric Design Language) routine in the environment of the ANSYS software to simulate the response of a moving force on an inclined Timoshenko beam. Then, the linear and nonlinear FEM solutions were compared with those obtained by the linear and nonlinear analytical solutions applying the mode summation technique. In the modeling of the Timoshenko beam we used BEAM-188

element defined in this software, which is suitable for analyzing beam structures. This element is a 2-D 2-noded second order beam element having 6 (or 7) DOFs with 3-translational DOF and 3-rotational DOF in each node. Now, to establish our calculations we consider an inclined undamped Timoshenko beam with geometry and mechanical properties listed in Table 1.

Table 1. Geometric and material properties of considered inclined beam [18]

Parameter	Symbol	Value
Beam's cross-sectional area (m^2)	$A\,(b \times h)$	$5 \times 10^{-3}\,(0.05 \times 0.1)$
Beam's length (m)	l	6
Young's modulus (N/m^2)	E	207×10^9
Shear modulus (N/m^2)	G	77.6×10^9
Beam's density (kg/m^3)	ρ	7850
Poisson's coefficient	ν	0.25
Shear correction factor	k	0.85
Gravitational acceleration (m/s^2)	g	9.81
Damping coefficient	η	0.033
Kinetic frictional coefficient	μ	0.2

Fig. 3 illustrates the variation of the mid-point deflection $w\,(m)$ of an inclined undamped pinned-pinned Timoshenko beam with $\varphi = 36^\circ$ vs. non-dimensional time vt/l at velocity ratio $\alpha = 0.25$ for the traveling force $F = 2\rho g A l$ (N) under influence of constant velocity motion using FEM analysis and analytical analysis, respectively. From this figure, one can conclude that the results for the beam's mid-point lateral dynamic displacement obtained by FEM and analytical solutions in either of the nonlinear or the linear analysis are almost the same, which shows very good agreement between these analytical results obtained via mode summation technique and FEM analysis. The suitable number of elements which has been used for the beam to converge the linear/nonlinear results is 80 elements.

4.3. Results and discussions. In the all following case studies data given in Ref. [18] as well as those beam listed in Table 1 are taken into consideration.

To clarify the results and in order to have a better insight on interpreting the variation of the obtained results we tried to present the results in dimensionless forms. So we begin with defining the dimensionless dynamic deflection $w(x_{\max}, t)/w_0$ and the dimensionless time parameter t/t_i, $i = 1, 2,$ and 3 where w_0 and $x_{\max}$ $(= x|_{w_{\max}})$ denote the maximum static deflection and the point on the beam that corresponds to this deflection, respectively. It should be noticed that $w(x_{\max}, t)$ is obtained from dynamic analysis of the governing equations of motion at $x_{\max}$. Table 2 shows the values of w_0 and position of $x_{\max}$ due to the lateral force, i.e., F, for three different types of the beam's boundary conditions.

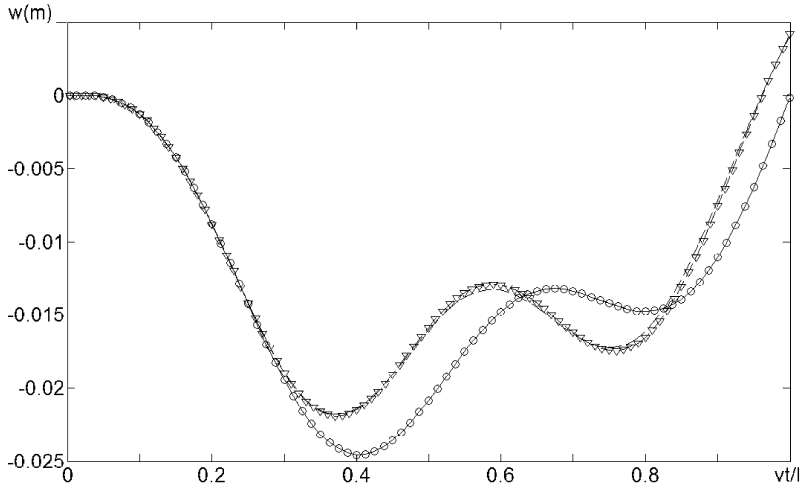

Fig. 3. Variation of mid-point deflection $w\,(m)$ vs. normalized time vt/l for an inclined pinned-pinned Timoshenko beam with $\varphi = 36^\circ$ affected by a moving force $F = 2\rho gAl(N)$ under constant velocity motion at $\alpha = 0.25$ using analytical and FEM analyses for linear and nonlinear solutions: $(-)$ analytical linear solution, $(- -)$ analytical nonlinear solution, $(-\circ-)$ ANSYS linear solution (80 elements used), $(-\triangledown-)$ ANSYS nonlinear solution (80 elements used).

Table 2. Values of $x_{\max}\ (=\ x|_{w_{\max}})$ and w_0 due to the applied lateral force F for different boundary conditions of a beam [2, 18]; (φ is the beam's inclination angle)

Beam geometry	B.C.s	Position of applied lateral force F; $x_{\max}(=\ x|_{w_{\max}})$	Absolute value of w_0
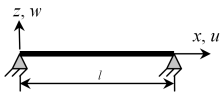	pinned-pinned	$x = 0.5l$	$w_0 = \frac{Fl^3\cos\varphi}{48EI_d}$
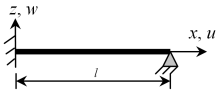	clamped-pinned	$x = 0.55l$	$w_0 = \frac{Fl^3\cos\varphi}{48\sqrt{5}EI_d}$
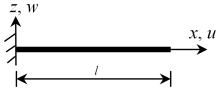	clamped-free	$x = l$	$w_0 = \frac{Fl^3\cos\varphi}{3EI_d}$

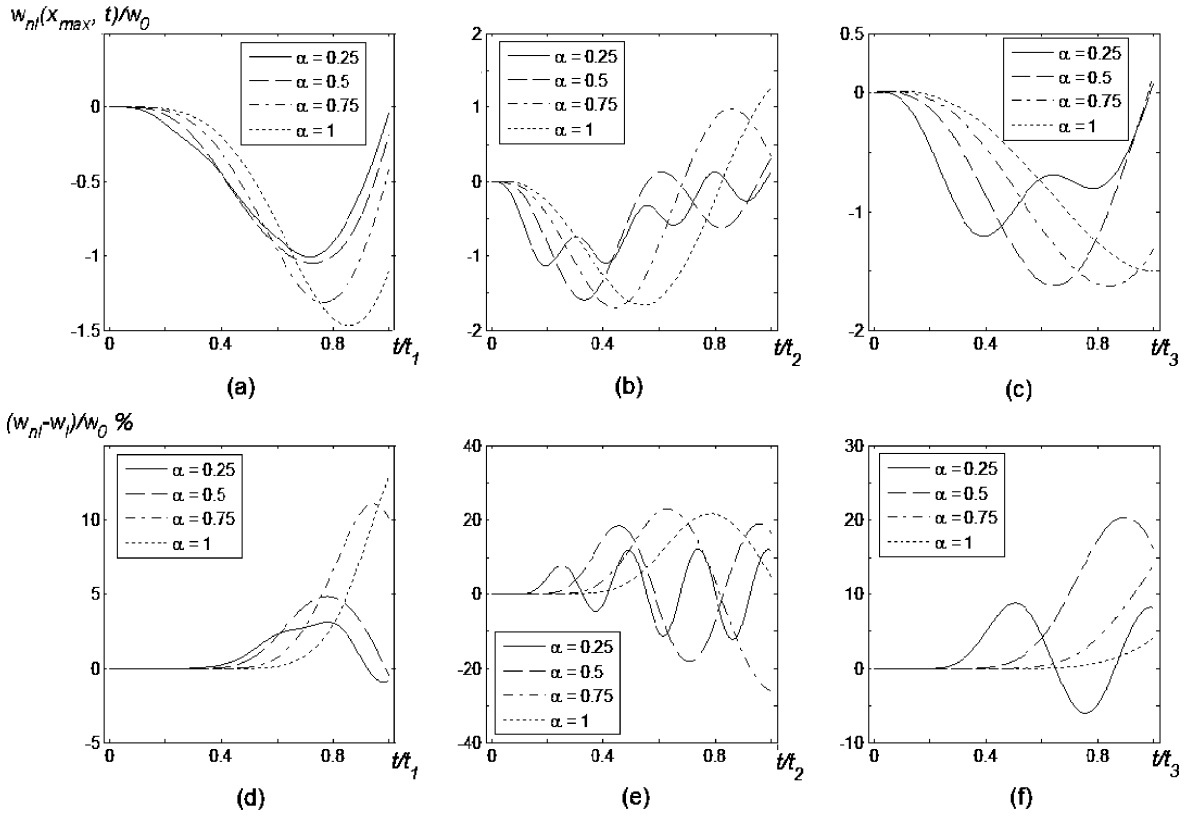

Fig. 4. Variation of dimensionless dynamic lateral deflection $(w_{nl}(x_{\max}, t)/w_0)$ at $x_{\max} = 0.5l$ vs. normalized time (t/t_i) for an inclined pinned-pinned Timoshenko beam ($\varphi = 30^\circ$) traversed by a moving force of $F = \rho g A l(N)$ with different velocity ratios ($\alpha = 0.25, 0.5, 0.75$ and 1) under influence of three types of motion; (a – c) dimensionless results for nonlinear analysis: $w_{nl}(x_{\max}, t)/w_0$, (d – f) dimensionless difference between nonlinear and linear analysis in percent: $(w_{nl} - w_l)/w_0$.

Moreover, let's define the velocity ratio as $\alpha = v/v_{cr}$. For a Timoshenko beam, v_{cr} is the critical velocity of a concentrated moving force on this beam defined in general form as $(v_{cr})_{\text{Timo}} = \omega_1 l/\pi$ [10, 11, 18], where ω_i is the any natural angular frequency (rad/s) of transversal/bending slope warping vibration of this beam given as: $(\omega_i)_{\text{Timo}} = \dfrac{b_i}{l^2}\sqrt{\dfrac{EI_d}{\rho A}}$ [18, 20] with $i = 1, 2, \ldots, n$ (see Eq. (26); also please see [10, 11, 18]. Note that b_i depends on the type of boundary condition and for example for a simply supported Timoshenko beam, $b_1 = \pi/B_1$, $b_i = i\pi/B_i$, $i = 1, 2, \ldots, n$; consequently the critical velocity of example first mode is $(v_{cr})_{\text{Timo}} = (1/lB_1)\sqrt{EI_d/\rho A}$ [10, 11, 18]. On the other hand, for only a simply supported kind of boundary condition a modified formula for $(v_{cr})_{\text{Timo}}$ is given in [15, 18]. For this case of boundary condition, the difference between $(v_{cr})_{\text{Euler}} = (\pi/l)\sqrt{EI_d/\rho A}$ [8, 10, 13, 18] and $(v_{cr})_{\text{Timo}}$ [10, 11, 15, 18] is about 0.03%. However, in general, we prefer to use $(v_{cr})_{\text{Timo}}$ [10, 11, 15, 18] in our up-coming calculations for each type of BC.

It should be mentioned that based on the previous analysis and obtained results which reveal that the friction force is very small [6], we neglect the effect of friction in the following case studies. Figs. 4 – 6 illustrate the variation of dimensionless dynamic lateral deflection $(w(x_{\max}, t)/w_0)$ vs. dimensionless time t/t_i, $i = 1, 2$ and 3, at reference point $x_{\max}$ $(= x|_{w_{\max}})$

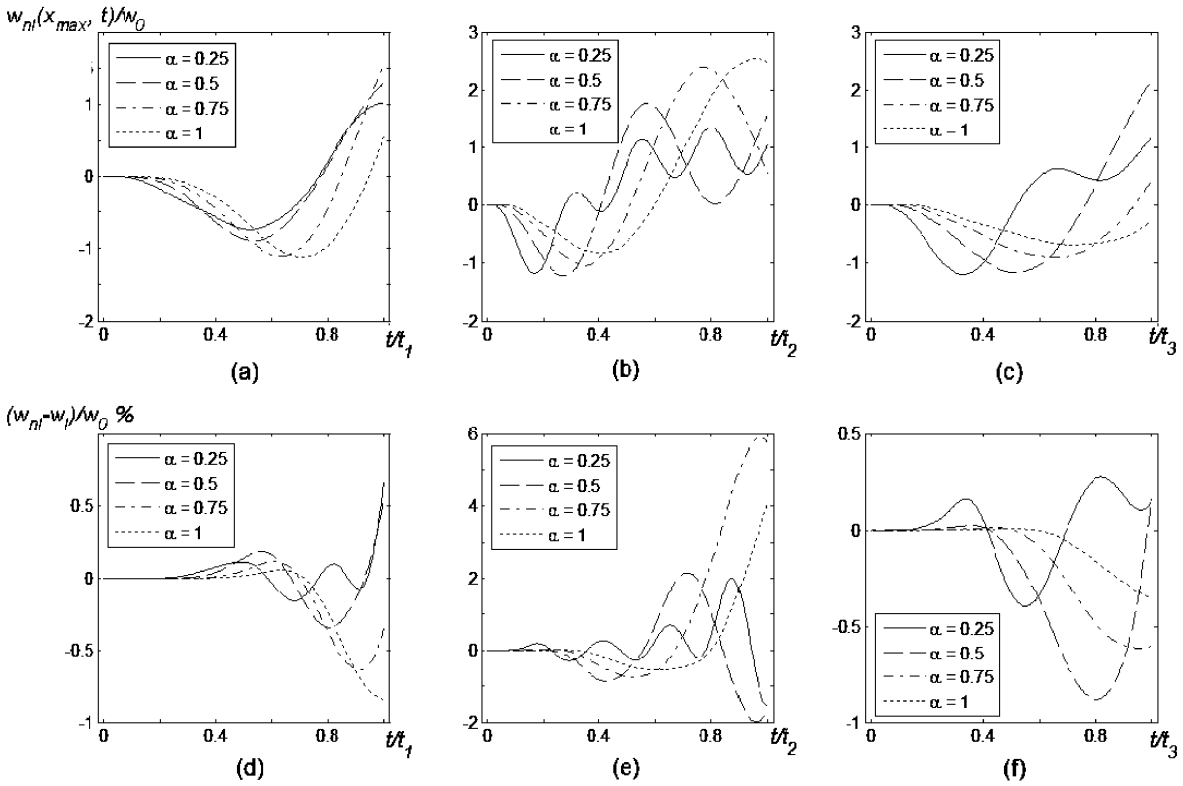

Fig. 5. Variation of dimensionless dynamic lateral deflection ($w_{nl}(x_{\max}, t)/w_0$) at $x_{\max} = 0.55l$ vs. normalized time (t/t_i) for an inclined clamped-pinned Timoshenko beam ($\varphi = 30^\circ$) traversed by a moving force of $F = \rho gAl(N)$ with different velocity ratios ($\alpha = 0.25, 0.5, 0.75$ and 1) under influence of three types of motion; (a – c) dimensionless results for nonlinear analysis: $w_{nl}(x_{\max}, t)/w_0$, (d – f) dimensionless ifference between nonlinear and linear analysis in percent: $(w_{nl} - w_l)/w_0$.

for pinned-pinned, clamped-pinned and clamped-free Timoshenko beam, respectively, with inclination angle $\varphi = 30^\circ$ traversed by a moving force $F = \rho gAl$ (N) with different velocity ratios ($\alpha = 0.25, 0.5, 0.75$ and 1) under influence of three types of motion. In the aforementioned figures, the depicted results on the left, middle and right columns are related to the cases of accelerating, decelerating and constant velocity motion, respectively. Moreover, in those figures, the first and the second rows show the dimensionless results obtained from the nonlinear analysis ($w_{nl}(x_{\max}, t)/w_0$) and percentage of dimensionless difference between the nonlinear and the linear analysis ($(w_{nl} - w_l)/w_0$), respectively.

As can be seen from Figs. 4(a – c) in the decelerating and uniform velocity types of motion, by increasing the velocity ratio α up to $\alpha = 0.75$ and $\alpha = 0.5$, respectively, the value of maximum dynamic deflection increases and decreases afterwards, respectively, whereas in the accelerating type of motion an increasing trend can be seen for the maximum dynamic deflecti-

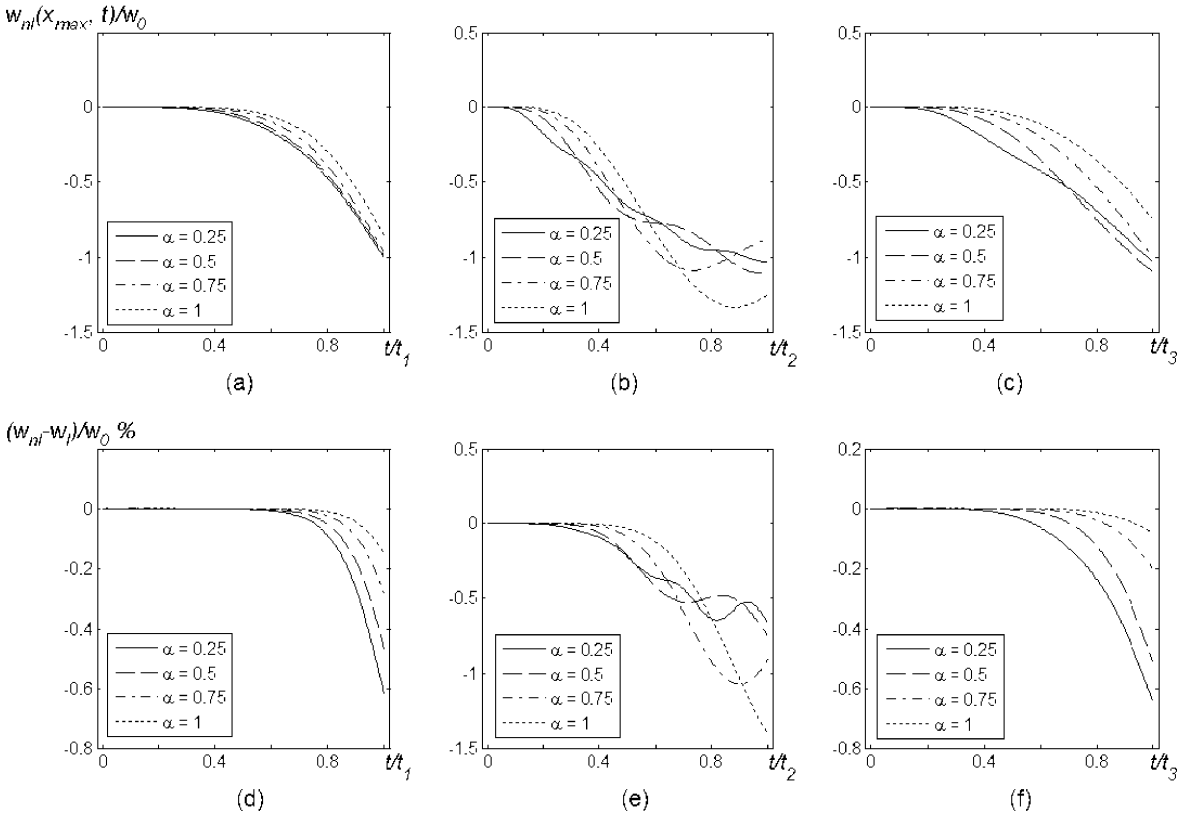

Fig. 6. Variation of dimensionless dynamic lateral deflection $(w_{nl}(x_{\max}, t)/w_0)$ at $x_{\max} = l$ vs. normalized time (t/t_i) for an inclined clamped-free Timoshenko beam $(\varphi = 30^\circ)$ traversed by a moving force of $F = \rho g A l(N)$ with different velocity ratios $(\alpha = 0.25, 0.5, 0.75$ and $1)$ under influence of three types of motion; (a – c) dimensionless results for nonlinear analysis: $w_{nl}(x_{\max}, t)/w_0$, (d – f) dimensionless difference between nonlinear and linear analysis in percent: $(w_{nl} - w_l)/w_0$.

on of the beam's mid-span. Moreover, in the decelerating type of motion the range of variation of the maximum dynamic deflection is larger with respect to other two types of motion. From Figs. 4(d – f), it is concluded that the maximum difference for the beam mid-span deflection between nonlinear and linear analysis happens primarily in the decelerating motion and with smaller difference in the case of uniform velocity and then in the accelerating type of motion, respectively.

It can be observed from Figs. 5(a – c) that in the accelerating type of motion by increasing the velocity ratio α the values of maximum dynamic downward deflection always increase, whereas in the decelerating and uniform velocity types of motion the value of maximum dynamic downward deflection increases up to $\alpha = 0.5$ and $\alpha = 0.25$, respectively, and decreases after these points. Also, it is seen from Fig. 5(a – c) that in the decelerating type of motion when the moving force is at the right end of the beam, i.e., $x = l$, the maximum dynamic upward (positive) deflection at $x_{\max} = 0.55\, l$ which happens at $\alpha = 1$ is the greatest value with respect to the other two types of motion. Moreover, it can be observed from Figs. 5(d – f) that the maximum difference at $x_{\max} = 0.55l$ for the beam deflection between nonlinear and linear analysis happens primarily in the decelerating motion and with smaller difference in the case of accelerating and then in the uniform velocity type of motion, respectively.

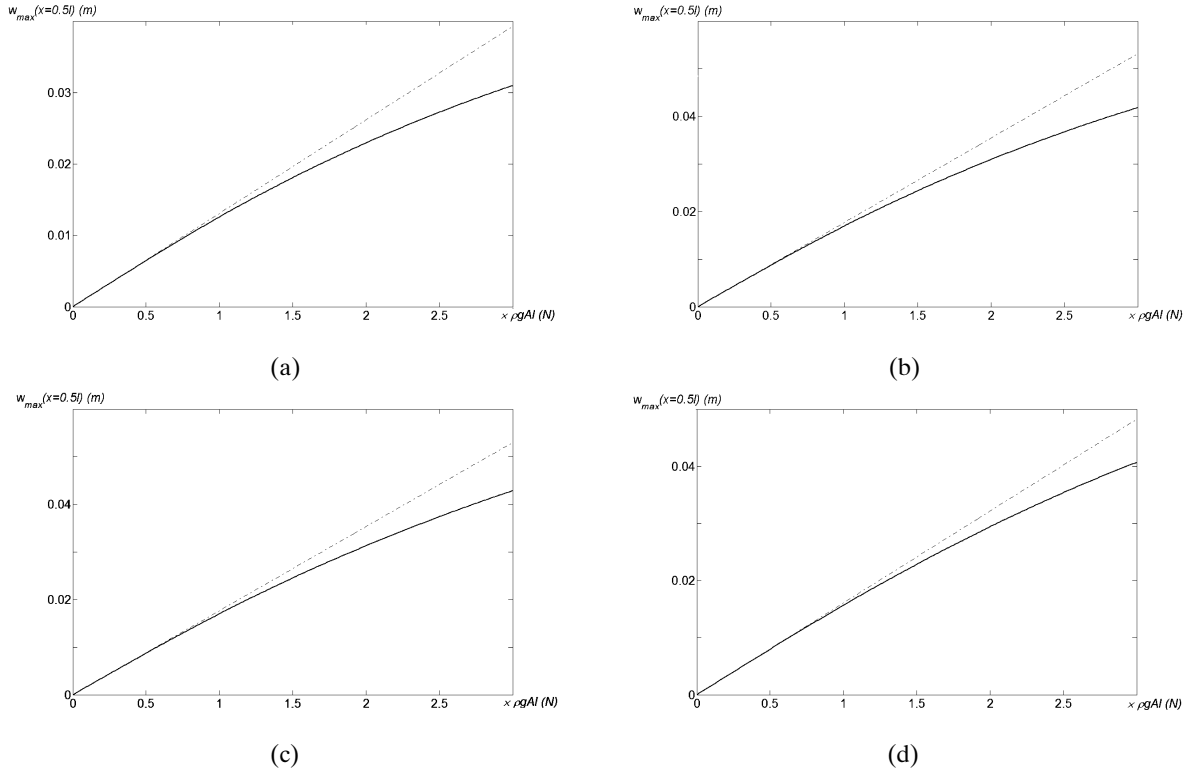

Fig. 7. Variation of the dynamic response of a point at $x = 0.5\,l$ of an inclined pinned-pinned Timoshenko beamvs. different values of the moving force for different velocity ratios in the uniform velocity motion; (a) $\alpha = 0.25$, (b) $\alpha = 0.5$, (c) $\alpha = 0.75$, (d) $\alpha = 1$; (—) nonlinear solution, (– · –) linear solution.

It can be observed from Figs. 6(a – c) that in the decelerating type of motion by increasing the velocity ratio α the value of maximum dynamic downward deflection at $x = l$ on the beam almost increases, whereas in the accelerating type of motion the reduction trend is always seen for the maximum dynamic downward deflection. Furthermore, in the uniform velocity type of motion by increasing the velocity ratio α up to $\alpha = 0.5$, the value of maximum dynamic downward deflection increases and vice versa afterwards. In addition, it can be observed from Figs. 6(d – f) that the maximum difference between nonlinear and linear analysis happens primarily in the decelerating motion and with smaller difference in the case of accelerating and then in the uniform velocity type of motion, respectively. Moreover, in this type of boundary condition, the differences are much lower than the one in the other two types of boundary conditions.

In Figs. 7 and 8 the absolute values of maximum dynamic response ($w_{\max}(x)$) variation of a point at $x = 0.5\,l$ and $0.55l$, respectively, on an inclined pinned-pinned and clamped-pinned Timoshenko beam with $\varphi = 30^\circ$ vs. different values of the moving force is shown for various velocity ratios of $\alpha = 0.25, 0.5, 0.75$ and 1, respectively, using both linear and nonlinear solutions in the uniform velocity type of motion, respectively. It can be seen from Fig. 7 that the maximum dynamic deflection of the nonlinear analysis is always lower than the one obtained from the linear solution. The hardening behavior is seen in this case as reported in other works [16, 18]. Also, the dynamic mid-point displacements of such beam using linear and nonlinear solutions are almost the same for the value of $F \leq 0.5\rho gAl(N)$. However, after this point,

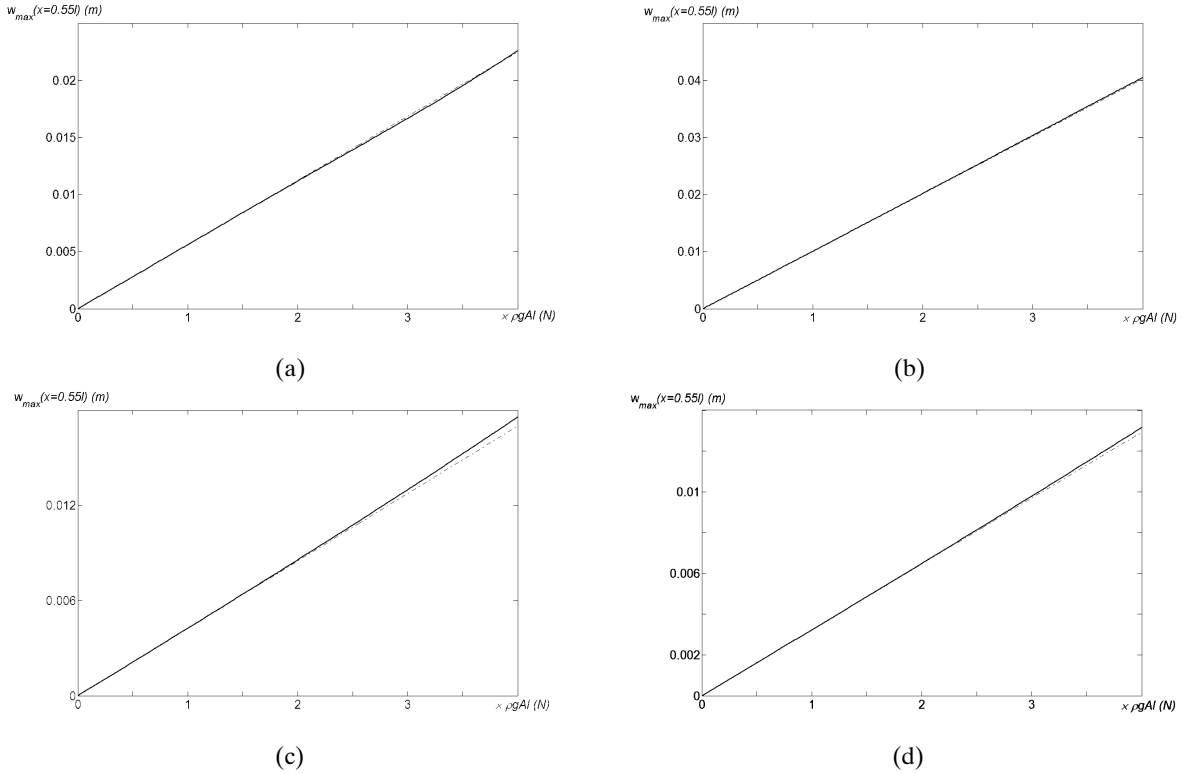

Fig. 8. Variation of the dynamic response of a point at $x = 0.55\,l$ of an inclined clamped-pinned Timoshenko beam vs. different values of the moving force for different velocity ratios in the uniform velocity motion; (a) $\alpha = 0.25$, (b) $\alpha = 0.5$, (c) $\alpha = 0.75$, (d) $\alpha = 1$; $(-)$ nonlinear solution, $(- \cdot -)$ linear solution.

the magnitude of the $w_{\max}$ of the nonlinear and the linear solutions differs gradually and the difference grows rapidly as the value of F increases. Furthermore, from Fig. 7, the difference between the linear and the nonlinear solutions has an increasing trend up to the load velocity ratio of $\alpha = 0.5$ and a reverse trend afterwards. The maximum difference between linear and nonlinear solutions for all cases in this figure occurs at $F = 3\rho g A l(N)$ at $\alpha = 0.5$ (see Fig. 7(b)). Also, the variation of the linear solution mathematically follows a linear trend in this figure [8, 16].

It can be observed from Fig. 8 that both the hardening (stiffening) behavior in the lower velocity ratio ($\alpha = 0.25$) and the softening behavior in the higher velocity ratios ($\alpha = 0.5, 0.75$ and 1) can be predicted in this type of boundary condition of the beam under the action of a moving force. Also, the absolute values of maximum dynamic deflection ($w_{\max}(x = 0.55l)$) of a point at $x_{\max} = 0.55\,l$ of an inclined clamped-pinned Timoshenko beam using linear and nonlinear solutions are almost the same no matter what values of F might be. In addition, the difference between the linear and the nonlinear solutions has a bit increasing trend up to the load velocity ratio of $\alpha = 0.75$ and a reverse trend afterwards. In other words, the comparison of results indicates that the trend of difference reduction between linear and nonlinear solutions in the clamped-pinned type is much faster than the pinned-pinned type of BC (compare Figs. 7 and 8). Besides, it should be noted that the maximum difference between linear and nonlinear

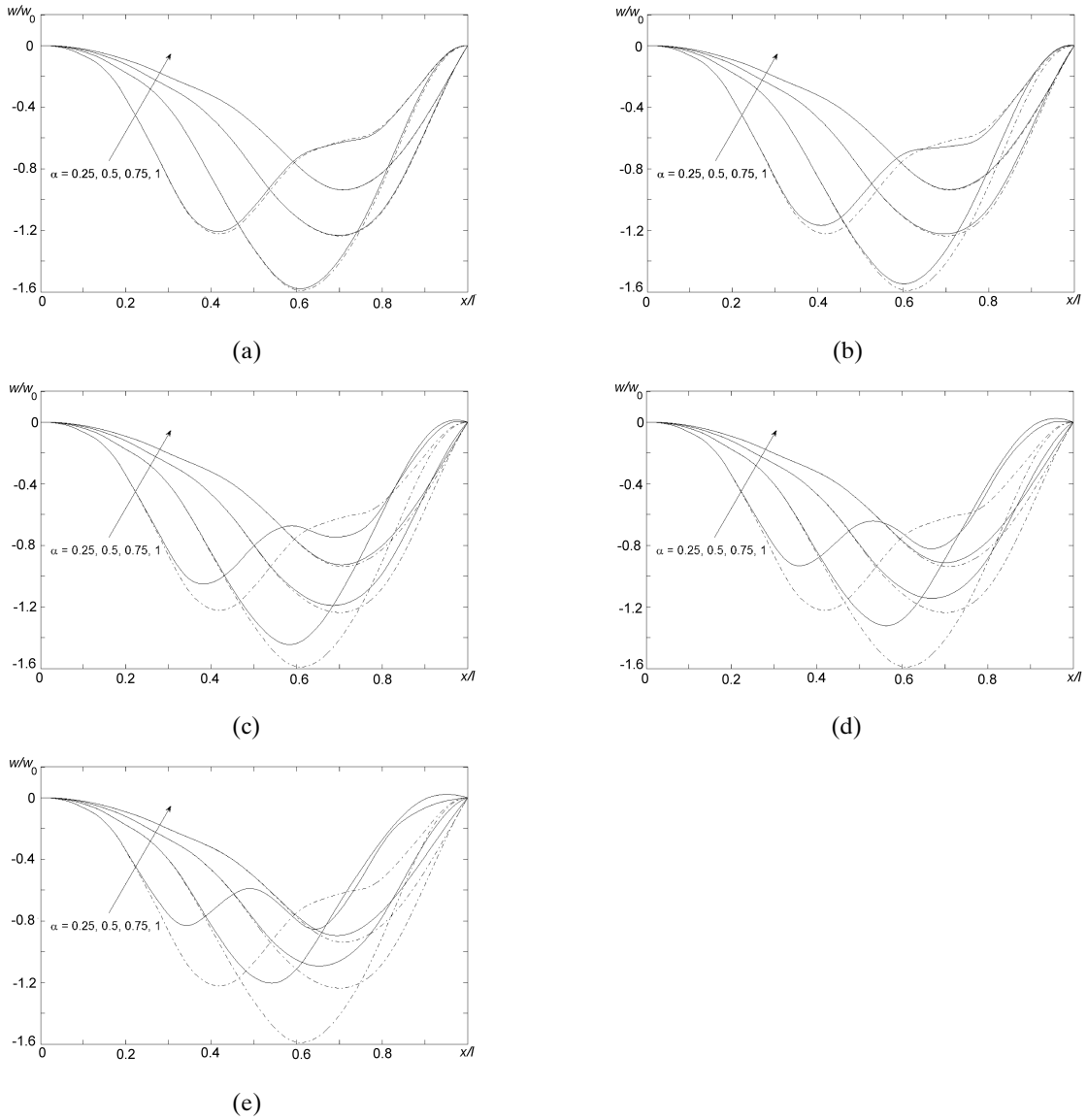

Fig. 9. Variation of dimensionless dynamic deflection (w/w_0) vs. (x/l) for an inclined pinned-pinned Timoshenko beam with $\varphi = 30^\circ$ at different velocity ratios for different moving force value of F in the constant velocity motion; (a) $F = 0.5\rho gAl(N)$, (b) $F = \rho gAl(N)$, (c) $F = 2\rho gAl(N)$, (d) $F = 3\rho gAl(N)$, (e) $F = 4\rho gAl(N)$; (—) nonlinear solution, (– · –) linear solution.

solutions for all cases in this figure occurs at $F = 4\rho gAl(N)$ at $\alpha = 0.75$ (see Fig. 8(c)). The variation of the linear solution mathematically also follows a linear trend in this type of BC.

It should be mentioned that for a clamped-free Timoshenko beam there is similar softening behavior (for brevity results are not illustrated here) with much less intensity compared to a clamped-pinned Timoshenko beam. It is believed that more pronounced reduction of softening/hardening behavior can be seen when supports are allowed to slide or to be free.

Using nonlinear and linear analysis in the case of constant velocity type of motion the variation of normalized lateral dynamic displacement (w/w_0) vs. x/l of an inclined pinned-pinned,

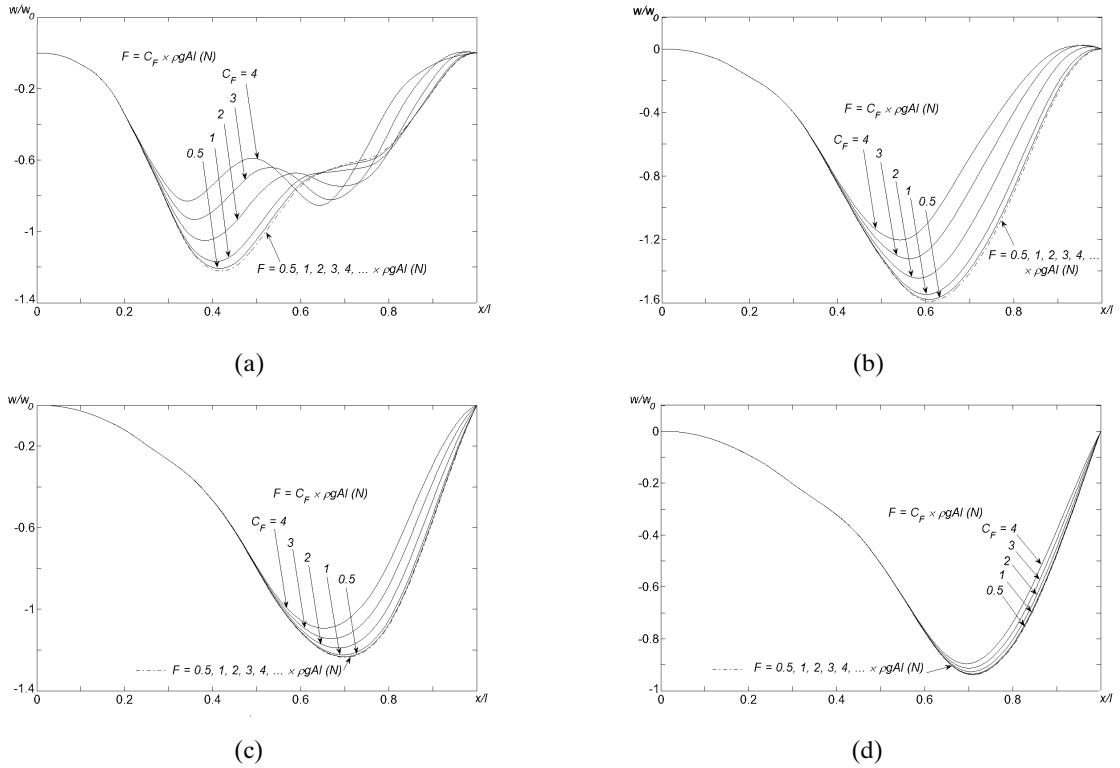

Fig. 10. Variation of dimensionless dynamic deflection (w/w_0) vs. (x/l) for an inclined pinned-pinned Timoshenko beam with $\varphi = 30^\circ$ at different moving force size of F for different velocity ratios in the constant velocity motion; (a) $\alpha = 0.25$, (b) $\alpha = 0.5$, (c) $\alpha = 0.75$, (d) $\alpha = 1$; (—) nonlinear solution, (– · –) linear solution.

clamped-pinned and clamped-free Timoshenko beam by changing velocity ratios, α, and moving force value, F, are shown respectively, in Figs. 9 – 10, 11 – 12 and 13 – 14.

It can be seen from Fig. 9 that the nonlinear analysis results of w/w_0 are almost lower than the one obtained from the linear analysis. Also, when α increases the difference between linear and nonlinear analysis decreases. This difference increases when the value of F increases. The maximum difference between linear and nonlinear analysis happens at $\alpha = 0.25$ when $F = 4\rho gAl$ (N). The linear solutions always predict a unique value of w/w_0 in the same velocity ratio of α no matter what values of F might be.

It can be seen from Fig. 10 that that for all velocity ratios α the linear analysis always has an identical value for w/w_0 no matter what the values of F are. Moreover, it is seen that the point corresponding to the $(w_{\max})_{\text{linear}}$ is always in right side of the similar point on the nonlinear analysis. And where the magnitude of moving force is small, i.e., $F = 0.5\,\rho gAl(N)$ the nonlinear and the linear solutions are almost the same no matter what the values of α might be. However, after this point ($F > 0.5\rho gAl(N)$) the difference between linear and nonlinear solutions becomes more pronounced, and consequently the difference between the linear and the nonlinear solution of maximum value of deflection increases accordingly. Furthermore, by increasing the velocity ratio up to $\alpha = 0.5$ the maximum dynamic deflection of linear and nonlinear solutions increases and the reverse trend prevails afterwards so that the maximum dynamic deflection of the linear and the nonlinear solutions occurs at $F = 4\rho gAl(N)$ at $\alpha = 0.5$.

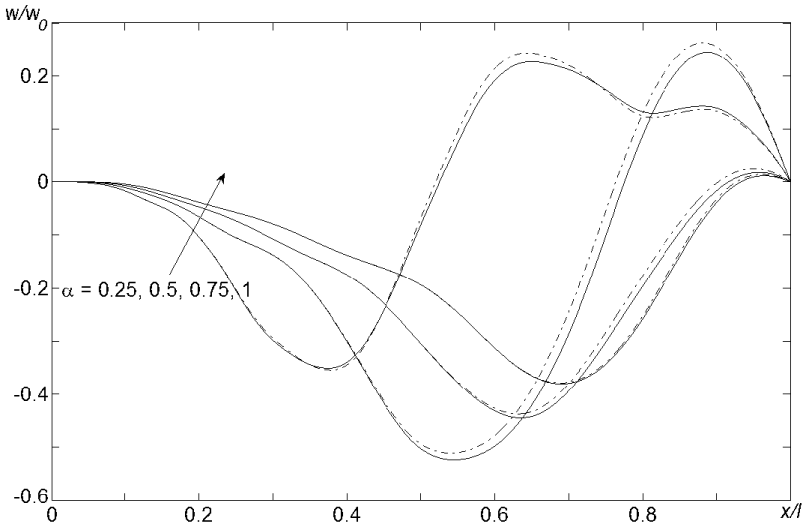

Fig. 11. Variation of dimensionless dynamic deflection (w/w_0) vs. (x/l) for an inclined clamped-pinned Timoshenko beam with $\varphi = 30^\circ$ at different velocity ratios for moving force value of $F = 4\rho gAl(N)$ in the constant velocity motion; (—) nonlinear solution, (– · –) linear solution.

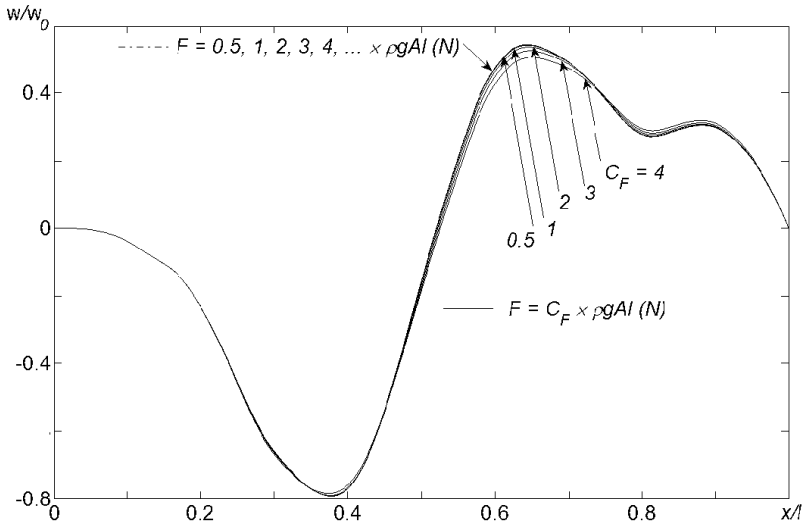

Fig. 12. Variation of dimensionless dynamic deflection (w/w_0) vs. (x/l) for an inclined clamped-pinned Timoshenko beam with $\varphi = 30^\circ$ at different moving force of F for velocity ratio $\alpha = 0.25$ in the constant velocity motion; (—) nonlinear solution, (– · –) linear solution.

It can be observed from Fig. 11 that the instantaneous dynamic deflection calculated from the nonlinear analysis is almost greater than the one obtained from the linear analysis. Also, Fig. 12 shows that the linear analysis always presents a unique value for w/w_0 no matter what values of F might be. Moreover, for small magnitude of moving force F, i.e., $F = 0.5\rho gAl(N)$,

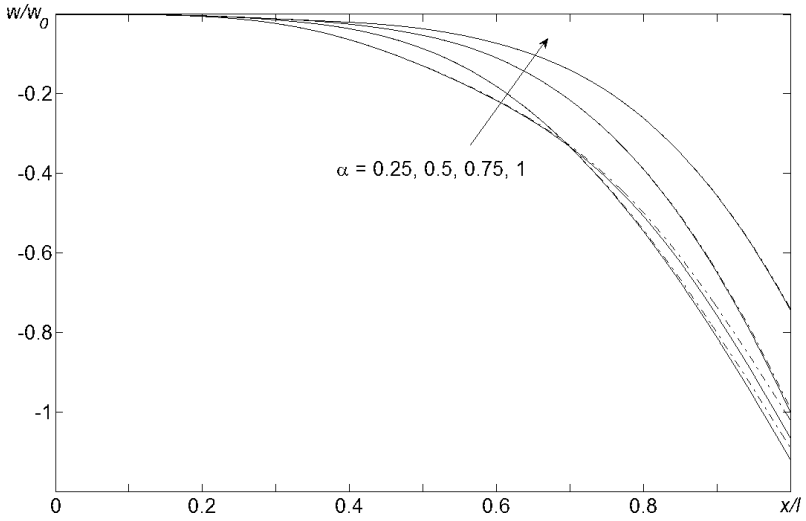

Fig. 13. Variation of dimensionless dynamic deflection (w/w_0) vs. (x/l) for an inclined clamped-free Timoshenko beam with $\varphi = 30^\circ$ at different velocity ratios for moving force value of $F = 4\rho gAl(N)$ in the constant velocity motion; (—) nonlinear solution, (– · –) linear solution.

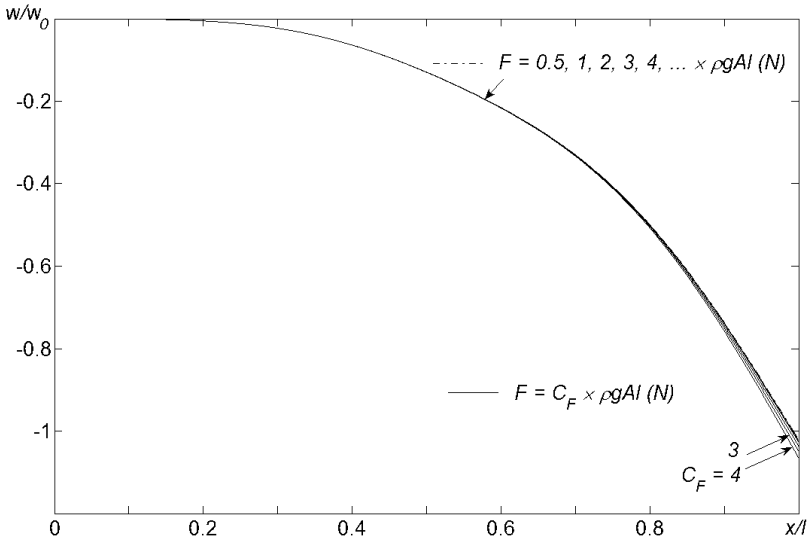

Fig. 14. Variation of dimensionless dynamic deflection (w/w_0) vs. (x/l) for an inclined clamped-pinned Timoshenko beam with $\varphi = 30^\circ$ at different moving force of F for velocity ratio $\alpha = 0.25$ in the constant velocity motion; (—) nonlinear solution, (– · –) linear solution.

the nonlinear and the linear solutions are almost the same. After this point ($F > 0.5\rho gAl(N)$) the difference between the linear and the nonlinear solution increases slightly. It can be observed from Figs. 13 and 14 that for the clamped-free beam the difference between the linear and the nonlinear analysis can be negligible graphically. However, the maximum difference between the linear and the nonlinear analysis occurs at $F = 4\rho gAl(N)$ at $\alpha = 0.25$.

5. Conclusions. Three nonlinear coupled partial differential equations of motion are solved for the rotation of warped cross section, longitudinal and transversal displacements of an inclined Timoshenko beam with different boundary conditions subjected to a moving force under influence of three types of motions including accelerating, decelerating and constant velocity motion, and the outcome results are the followings:

In the pinned-pinned and the clamped-pinned types of boundary condition under influence of accelerating type of motion, the maximum dynamic deflection is reached at much later time than the other two cases. Moreover, in the decelerating type of motion the range of variation of maximum dynamic deflection is greater than the one obtained from other two types of motion for all types of boundary conditions of the beam.

It is concluded that the maximum difference between nonlinear and linear analysis for the beam deflection at a reference point, i.e., $x_{\max}$ $(= x|_{w_{\max}})$ almost happens primarily in the decelerating motion and with smaller difference in the case of accelerating and then in the uniform velocity types of motion, respectively.

The maximum dynamic displacements of a moving force problem using linear and nonlinear solutions are almost the same for lower values of F. However, for larger values of F, the magnitude of the beam deflection of the nonlinear and the linear solutions differs gradually and the difference grows rapidly as the value of F increases. Also, by increasing the velocity ratio the difference between linear and nonlinear solution of maximum dynamic deflection of the beam becomes negligible. In addition, for pinned-pinned, clamped-pinned and clamped-free types of boundary condition the variation of the linear solution mathematically follows a linear trend in a moving force problem.

From the nonlinear analysis point of view, due to the existence of the quadratic-cubic nonlinearity nature of the governing coupled PDEs of motion, in a pinned-pinned Timoshenko beam the system behaves like a hard spring. That is, by increasing the magnitude of the moving force, the dynamic deflections become smaller than those from solution of linear system whereas in the clamped-pinned and clamped-free types of boundary conditions, the system behaves like a hard/soft and soft spring, respectively. For a soft system by increasing the magnitude of the moving force, the nonlinear dynamic deflection becomes greater than those obtained from the linear solution.

When α increases, the value of maximum instantaneous dynamic deflection decreases so that for higher velocity ratios, i.e., $\alpha = 0.75$ and 1, the values of linear and nonlinear solutions are almost the same no matter what values of F might be. Furthermore, by increasing the magnitude of moving force F the difference between maximum value of the linear and the nonlinear solution increases.

It can be observed that the linear solution of the instantaneous dynamic deflection under a moving force always shows a unique value in any identical value of the velocity ratio α no matter what values of F might be, whereas this behavior can not be seen in the nonlinear analysis.

1. *Michaltsos G. T.* Dynamic behavior of a single-span beam subjected to loads moving with variable speeds // J. Sound and Vibration. — 2002. — **258**, № 2. — P. 359 – 372.

2. *Abu Hilal M., Zibdeh H. S.* Vibration analysis of beams with general boundary conditions traversed by a moving force // J. Sound and Vibration. — 2000. — **229**, № 2. — P. 377 – 388.

3. *Lin Y. H., Trethewey M. W.* Finite element analysis of elastic beams subjected to moving dynamic loads // J. Sound and Vibration. — 1990. — **136**, № 2. — P. 223 – 242.

4. *Xu X., Xu W., Genin J.* A non-linear moving mass problem // J. Sound and Vibration. — 1997. — **204**, № 3. — P. 495 – 504.
5. *Olsson M.* On the fundamental moving load problem // J. Sound and Vibration. — 1991. — **145**, № 2. — P. 299 – 307.
6. *Wu J. -J.* Dynamic analysis of an inclined beam due to moving loads // J. Sound and Vibration. — 2005. — **288**. — P. 107 – 133.
7. *Kiani K., Nikkhoo A., Mehri B.* Prediction capabilities of classical and shear deformable beam models excited by a moving mass // J. Sound and Vibration. — 2009. — **320**. — P. 632 – 648.
8. *Mamandi A., Kargarnovin M. H., Younesian D.* Nonlinear dynamics of an inclined beam subjected to a moving load // Nonlinear Dynamics. — 2010. — **60**. — P. 277 – 293.
9. *Yanmeni Wayou A. N., Tchoukuegno R., Woafo P.* Non-linear dynamics of an elastic beam under moving loads // J. Sound and Vibration. — 2004. — **273**. — P. 1101 – 1108.
10. *Fryba L.* Vibration of solids and structures under moving loads. — London: Thomas Telford Publ., 1999.
11. *Fryba L.* Dynamics of railway bridges. — London: Thomas Telford Publ., 1996.
12. *Mamandi A., Kargarnovin M. H., Younesian D.* Nonlinear vibrations of an inclined beam subjected to a moving load // J. Phys. Conf. Ser. 181, 012094, doi: 10.1088/1742-6596/181/1/012094 (2009).
13. *Lee H. P.* The dynamic response of a Timoshenko beam subjected to a moving mass // J. Sound and Vibration. — 1996. — **198**, № 2. — P. 249 – 256.
14. *Wang R. T., Chou T. H.* Non-linear vibration of Timoshenko beam due to moving force and the weight of beam // J. Sound and Vibration. — 1998. — **218**, № 1. — P. 117 – 131.
15. *Sniady P.* Dynamic response of a Timoshenko beam to a moving force // J. Appl. Mech. Trans. ASME. — 2008. — **75**. — P. 024503-1 – 024503-4.
16. *Mamandi A., Kargarnovin M. H.* Dynamic analysis of an inclined Timoshenko beam travelled by successive moving masses/forces with inclusion of geometric nonlinearities // Acta Mech. — 2011. — **218**, № 1. — P. 9 – 29.
17. *Mamandi A., Kargarnovin M. H.* Nonlinear dynamic analysis of an inclined Timoshenko beam subjected to a moving mass/force with beam's weight inclined // Shock and Vibration. — 2011. — **18**, № 6. — P. 875 – 891.
18. *Mamandi A., Kargarnovin M. H., Farsi S.* An investigation on effects of traveling mass with variable velocity on nonlinear dynamic response of an inclined Timoshenko beam with different boundary conditions // Int. J. Mech. Sci. — 2010. — **52**, № 12. — P. 1694 – 1708.
19. *Nayfeh A. H., Mook D. T.* Nonlinear oscillations. — New York: Wiley-Intersci., 1995.
20. *Karrnovsky I., Lebed O. I.* Formulas for structural dynamics. — McGraw-Hill, 2001.
21. *Rao S. S.* Mechanical vibrations. — New York: Addison-Wesley, 2000.

Received 16.12.11,
after revision — 10.07.12